TÜBİTAK

Turkish Journal of Earth Sciences

http://journals.tubitak.gov.tr/earth/

Research Article

Turkish J Earth Sci
(2022) 31: 438-451

doi:10.55730/1300-0985.1812

A history of *Pistacia lentiscus* and *Pinus brutia* trees and their ecological changes in the Güllük Bay (Muğla, SW Turkey) during the last 400 years

Demet BİLTEKİN[1,*], Georg SCHWAMBORN[1], Kürşad Kadir ERİŞ[2], Dursun ACAR[1,2], Bikem EKBERZADE[1], Zahra HASHEMI[1], Nurettin YAKUPOĞLU[2], Ali MOHAMMADI[1], Ömer YETEMEN[1,3]

[1]İstanbul Technical University, Eurasia Institute of Earth Sciences, İstanbul, Turkey

[2]İstanbul Technical University, Eastern Mediterranean Centre for Oceanography and Limnology (EMCOL), Faculty of Mining, Department of Geological Engineering, İstanbul, Turkey

[3]School of Engineering, The University of Newcastle, Callaghan, New South Wales, Australia

Received: 22.12.2021 • **Accepted/Published Online:** 04.07.2022 • **Final Version:** 09.09.2022

Abstract: In this study, we present pollen records together with a multiproxy analysis from a sediment core collected from the Güllük Bay (Bargilya Cove, Muğla, SW Turkey), covering the last 400 years. Pistachio shrubland was occupying around the Güllük Bay between 1613 and 1741 AD. However, after 1741 AD, the vegetation canopy suddenly changed and Turkish pine (*Pinus brutia*) was established. This supports that the main factor affecting the expansion of *Pistacia lentiscus* was precipitation rather than temperature after 1741 AD. This change is also indicated by high Sr-Ca values, reflecting arid conditions. Two anthropogenic phases developed in the region. The first phase is marked by *Olea europeae* between 1613 and 1789 AD. The second is characterized by *Plantago*, Caryophyllaceae, *Cerelia*, *Rumex*, and *Sanguisorba minor* type suggesting pastoralism and agricultural activities between 1789 and 1964 AD. Macrofaunal communities are also indicative of environmental changes. *Abra ovata*, *Cerastoderma glaucum*, *Bittium reticulatum*, and *Skenea catenoides* were first settlers between 1572 and 1643 AD. The prominent presence of lagoonal species *Abra ovata* and *Hydrobia ventrosa* indicates a lagoonal depositional environment in 1799-1948 AD.

Key words: Pollen analysis, paleoclimate, paleovegetation, XRF, PCA, gastropods, molluscs

1. Introduction

Coastal lagoons constitute 13% of the world's coastal areas, which are dynamic and productive ecosystems (Nixon, 1982; Kjerfve, 1994; Conde et al., 1999). These lakes provide enormous biological resources and life support services, and they play important role in supporting the human's well-being. Various studies have been carried out in the lakes of Anatolia in terms of detailed interdisciplinary studies revealing how paleoecological and paleoclimatological changes affected the Eastern Mediterranean realm (Wick et al., 2003; Jones et al., 2007; Roberts et al., 2008; Litt et al., 2009; Kuzucuoğlu et al., 2011; Roberts et al., 2011a, 2011b; Ülgen et al., 2012; Eriş et al., 2013; Eriş et al., 2018, Biltekin et al., 2018; Biltekin et al., 2021). The Eastern Mediterranean basin has a long history in human history and is a unique study area to explore the interactions between climate, environment, and human activities (Roberts, 2014). The basic approach of multidisciplinary studies is to identify the duration of the paleoclimatic changes and their impacts on the paleoenvironment. Paleoclimate studies conducted in the Anatolian lakes show that the climate was wetter and colder during the late Pleistocene and Holocene than today (Wick et al., 2003; Jones et al., 2007; Fleitmann, 2009; Litt et al., 2009; Woodbridge and Roberts, 2011; Luterbacher, 2012; Ülgen et al., 2012; Eriş, 2013; Ocakoğlu et al., 2013; Çağatay et al., 2014; Dean et al., 2015; Karlıoğlu Kılıç et al., 2018; Danladi et al., 2021).

The scarcity of continuous high-resolution climate and vegetation records and the inadequacy of multiproxy paleoclimate data hinder the understanding of the climate and vegetation history. For this reason, a multiproxy study of Bargilya Cove sediments located in the Güllük Bay (southwest Turkey) can provide a representative record of paleoclimate and paleoecological change over several centuries back in time.

Various studies based on pollen analysis have been carried out on lake sediments to determine paleovegetation and paleoclimate changes in Turkey (van Zeist et al., 1975; van Zeist and Woldring, 1978; Bottema and Woldring, 1984; Sullivan, 1989; van Zeist and Bottema, 1991; Bottema, 1995; Eastwood et al.,

* Correspondence: biltekin@itu.edu.tr

1999; Karadaş, 2013, Kamar, 2018; Karlıoğlu Kılıç et al., 2018; Biltekin et al., 2018, 2021; Danladi et al., 2021). For instance, the pronounced changes in vegetation during the last 20 thousand years have been revealed based on the pollen records of Karamık Swamp and Lake Söğüt in southwest Turkey (van Zeist et al., 1975). According to van Zeist et al. (1975), the climate was dry in southwest Turkey in the period between 20 and 14 thousand years before present (BP), and steppe vegetation dominated under arid conditions. After 12,000 years BP, the climatic conditions became unfavourable for tree growth, and forest vegetation began to develop significantly only after 8500 years BP. Today's vegetation began to form after 6000 BP. From 6000 to 3000 years BP, human effects on vegetation were hardly detected. However, many pollen diagrams of the Middle-Late Holocene, indicate a significant change that took place during 3000 years BP (van Zeist et al., 1975). Palynology is a significant tool to detect the changes in vegetation and climate. Therefore, we present here a pollen analysis that is combined with other proxies to evaluate paleoenvironmental conditions since the 16th century in a coastal lagoon (Muğla, SW Turkey) in the Aegean Sea coast. In this study, we also provide a piece of information on the mollusc fauna of the Güllük Bay contributing to the knowledge of the molluscan fauna of the study area and involving their ecological features.

1.1. Study area

The Bargilya Cove is located in the Güllük Bay on the southern coast of the Aegean Sea. It is included within the Bargilya Wetland with Metruk Tuzlası and Kocadere (Mazı) Creek (Figure 1). Bargilya Cove is a shallow hypersaline lagoon, and its maximum depth reaches 1.5 m (Altınsaçlı et al., 2015). The surface area of saltpan is 311 ha (hectare) (Altınsaçlı et al., 2015). The present-day vegetation of Bargilya Cove is represented by *Juncus acutus* (Spiny rush), *Salicornia europea* (Glasswort), *Sporobolus virginicus* (Saltwater couch), *Anthemis tomentosa* (Chamomile), *Plantago lagopus* (Mediterranean plantain), *Asphodelus aestivus* (Summer Asphodel) (Akyol, 2009), *Olea europaea* (Olive), *Pinus halepensis* (Aleppo pines), and tamarisk plants (Altınsaçlı et al., 2015). The Bargilya Cove is under the influence of the Mediterranean climate. According to the climate classification of the Turkish State Meteorological Service in Turkey, it has a semiarid to semihumid climate. While summers are hot and dry, winters are mild and rainy. During winter, it rarely snows on the peaks of a few high mountains. In summer, the average temperature is between 32 °C and 34 °C, and sometimes even exceeding 40 °C. In winter, the average temperature is 12–14°C, although it is rarely seen below 0 °C (http://www.milas.gov.tr/milasin-tarihcesi).

2. Materials and methods

2.1. Core collection

The studied core K3-1 (37°11′53.5266′′N, 27°35′17.16245′′E) was collected during the beginning of the autumn season in 2020 using a hand corer from a water depth of ca. 1 m at the lagoon's western margin (Figure 1). The core was stored at +4 °C in the core repository at the Eastern Mediterranean Centre for Oceanography and Limnology (EMCOL) in İstanbul Technical University (İTU). In order to get a clear view of the core before analyses, the core was split lengthwise into two halves using a cutting tool on the splitting table in the laboratory.

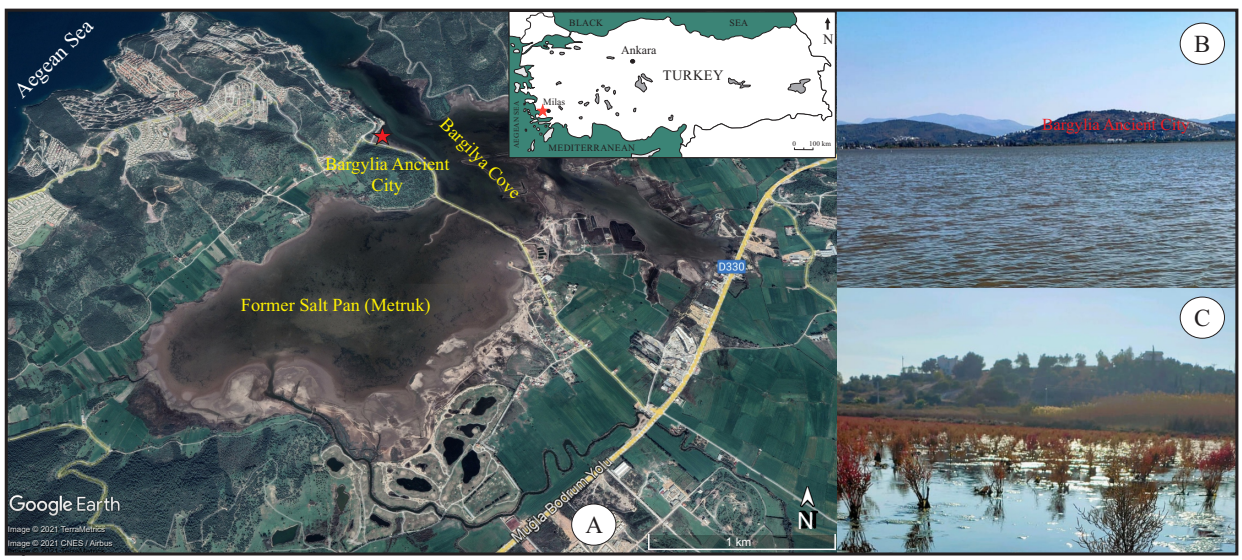

Figure 1. A. Location map of the study area with inlet map. **B.** General view from the coring site. **C.** *Salicornia herbacea* (common glasswort) in the Bargilya Cove (Muğla, Turkey). Photo: Bikem Ekberzade

After opening the core, its surface has been cleaned and smoothed in order to distinguish the different colours and to better define the sedimentary structures. Next to this, the cores have been photographed, lithologically described, and sampled for analyses.

2.2. µ-XRF analysis

Following core splitting, firstly the nondestructive analyses were carried out by using the Itrax µ-XRF Core scanner, which is equipped with XRF-EDS, X-Ray radiography, and RGB colour camera at the ITU-EMCOL Core Analyses Laboratory. A fine-focus Mo X-ray tube was used for the measurement. The X-ray generator was performed at 30 kV and 50 mA with a counting time of 20 s. The step-size interval was 0.5 mm. Element data from the core scanning device are semiquantitative data expressed as total counts (cps). This denotes the number of total counts collected by the detector during the measurement time for each step.

The elemental detection limits of XRF are robust for a spectrum of medium-heavy and lighter elements; i.e. Si, Al, S, Cl, K, Ca, Ti, Fe, As, Pb, Zn, Br, Rb, Sr, Zr, and Ba following Croudace et al. (2006). Calcium (Ca) is used here as a proxy of endogenic carbonate production and has been previously used in numerous marine and lacustrine environments (e.g., Cohen, 2003; Çağatay et al., 2014, 2015). Strontium (Sr) is an indicator of aragonite mineral in carbonate shells, the Sr-Ca ratio is an indicator of paleosalinity and paleotemperature in marine carbonates (e.g., Russell et al., 2004; Schöne et al., 2011). The Ca-Ti ratio is used for normalization from carbonate or siliciclastic sedimentation (Eriş et al., 2017).

We also make use of the Compton (incoherent) and Rayleigh (coherent) scattering (inc/coh) ratios as a proxy for LOI (loss-on-ignition), and TOC (total organic carbon) as examined by Chawchai et al. (2016). It is noteworthy that wet and organic-rich sediment material may be associated with poorer detection limits caused by the less efficient excitation of elements because of increased scattering (Croudace et al., 2006). The XRF data are of compositional nature, which means that they are vectors of nonnegative values subjected to a constant-sum constraint (usually 100%). This implies that relevant information is contained in the relative magnitudes, and geochemical data analyses can focus on using the ratios between components (Aitchison, 1990). Before PCA (principal component analysis), a centered log-ratio (clr) transformation was applied to the data set following Aitchison (1990).

2.3. Geotek Multi-Sensor Core Logger (MSCL) analysis

Physical properties, magnetic susceptibility (MS), and gamma density were measured at 1 cm resolution according to the standard procedures, using a Geotek Multi-Sensor Core Logger (MSCL) (Weaver and Schultheis, 1990).

2.4. Chronology

Radiocarbon dating was carried out on two gastropods and molluscs (*Bittium reticulatum* and *Abra ovata*) at the TÜBİTAK-MAM (Earth and Marine Sciences Institute) by using the Accelerated Mass Spectroscopy Laboratory (Table 1). Firstly, the samples were washed in distilled water and dried (at 60 °C) before the analysis. In this study, an age-depth model was constructed using the Clam.r (classical age-modelling) script, a non-Bayesian method. The Clam.r script has been operated by RStudio on calibrated ages to obtain accumulation histories in age-depth iterations (Blaauw, 2010). Therefore, the script has generated a cubic spline age-depth model with 95% Gaussian confidence interval (Figure 2). Clam.r (classical age-modelling) calibrated the uncalibrated ages using Marine20 calibration curve (Reimer et al., 2020) with 58 ± 85 ^{14}C year reservoir correction (Reimer and McCormac, 2002), and constructs the age-depth model between the calibrated ages by Markov chain Monte Carlo iterations. We present the ages and their corresponding 95% confidence intervals in Table 1, since they are used as ages for the dated depths.

2.5. Sampling and identification of pollen and spore grains

Approximately, 20 grams of sediment are taken from the core. The samples are prepared according to the standard pollen preparation method (Cour, 1974). First, 35% cold HCl acid and 47% cold HF acid are added to eliminate carbonate and silica content respectively. Then, $ZnCl_2$ (density>2.0) is used to separate palynomorphs. The resting sediments are sieved using 200 µm and 10 µm nylon sieves. The final residue is mounted on glass with one drop

Table 1. AMS radiocarbon calibrated ages (based on Marine20) of gastropod and bivalvia in the core K3-1 (cmbls: centimeters below lake surface).

Lab code	Material	Name	Core name	Core depth (cmbls)	Uncalibrated radiocarbon ages (BP)	Calibrated median ages (cal AD)
(TÜBİTAK-1794)	Gastropod	*Bittium reticulatum*	K3-1	8–9	1.1218 ± 0.0030 (F14C)	1993–1996
(TÜBİTAK-1793)	Gastropod and Bivalvia	*Bittium reticulatum, Abra ovata*	K3-1	28–30	402 ± 23	1572

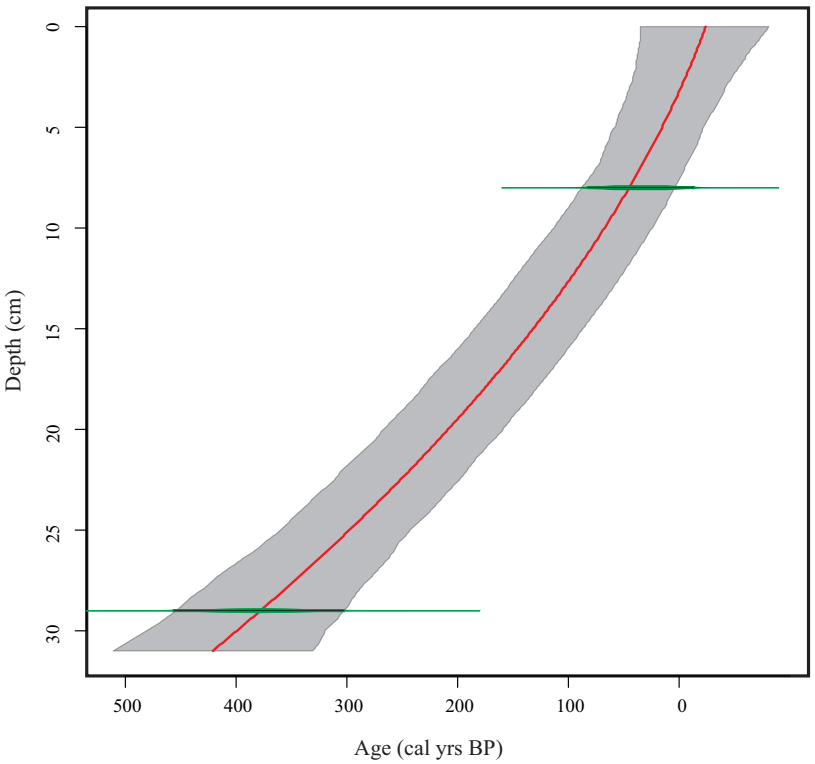

Figure 2. Age-depth model for core K3-1 by using R-studio and the script "Clam" (Blaauw, 2010).

of glycerin and fixed by a cover glass. Pollen grains are robust bioindicators (proxy) because the outer wall of the pollen, called exine, is resistant to all kinds of weathering effects and any acids. Plants generally show distribution according to temperature and precipitation changes. For this reason, pollen analysis allows the determination of climate changes in the past. Another feature of pollens is their morphological diversity. Each plant has its unique pollen morphology. This diversity makes it possible to make taxonomic studies by considering pollen grains. Palynological slides are studied under a light transmission microscope (Leica) at the Eurasia Institute of Earth Sciences Microscope Laboratory in İTU, using immersion oil with different lenses (×63 and ×100). Pollen counts are included between 300 and 500 pollen grains (excluding *Pinus*) per sample. Because *Pinus* generally produces a large amount of pollen, it can be easily transported and spread in water and air. The percentage of pine has been calculated according to the total pollen sum.

We used pollen atlases (Reille, 1992) and pollen photographs for pollen identification. The results are displayed in a detailed pollen diagram using the TiliaIT program (version 2.0.41; Grimm, 1991–2015, TiliaIT. https://www.tiliait.com). Pollen zones are determined in the TiliaIT program based on CONISS (constrained incremental sum-of-squares cluster analysis; Grimm, 1987) analysis and changes in pollen species. In addition to pollen and plant spores, nonpollen palynomorphs (NPP), such as fungal spores and algae, were identified and counted. For NPP identification, we used the published and reported images (van Geel et al., 2006; Cugny et al., 2010; Gelorini et al., 2011).

2.6. Paleontological analysis

Samples were washed and sieved with a 63-µm sieve for paleontological study. Following sieving, the samples were dried in an oven at 60 °C. Fossils (molluscs and gastropods) were identified under an Olympus SZX10 binocular microscope for detailed taxonomic observations. The preservation of molluscs and gastropod shells was found to be good, and specimens were photographed using an Olympus SZX10 microscope that was equipped with an Olympus digital camera (Plate I).

3. Results

3.1. Lithology and physical properties of the core

Two lithological units are distinguished in the core K3-1 based on visual description. Unit-1 (1925–1974 AD) is between 0and 6 cm, consisting of greenish homogenous mud, including marine and lagoonal molluscs and gastropods (Figure 3). Further down Unit-2 (1925-1551 AD) is between 6 and 30 cm depth, including a gray-

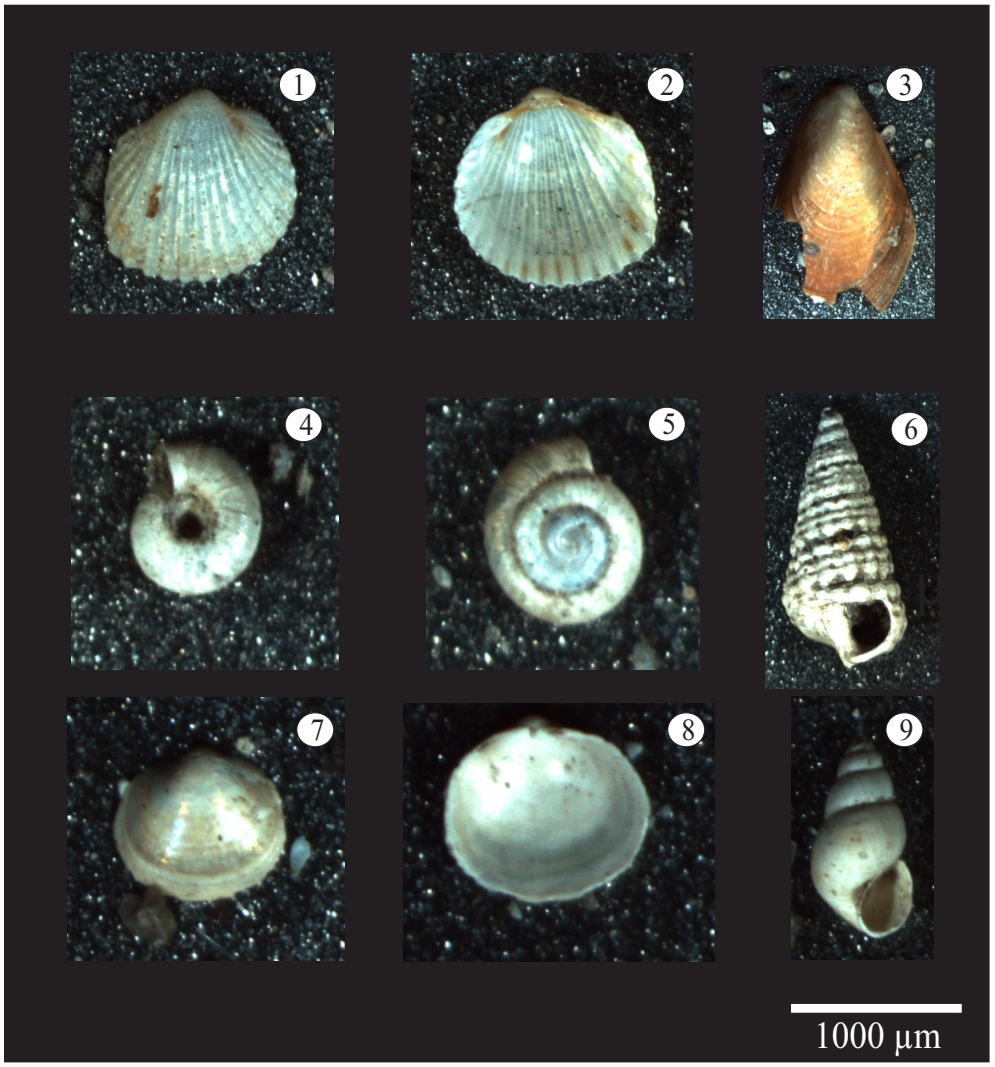

Plate I. 1–2: *Cerastoderma glaucum*; **3:** *Mytilus galloprovincialis*; **4–5:** *Skenea catenoides*; **6:** *Bittium reticulatum*; **7–8:** *Abra ovata*; **9:** *Hydrobia ventrosa*.

greenish mud. Within this unit, black spots appear at 20 cm depth with mm-scale in the core. Black reduced sediment surfaces (black spots) may indicate an elevated sulphide concentrations and low redox potentials at this level in the core. Although magnetic susceptibility (MS) values indicate high fluctuations along the core, this upper short interval (Unit-1: 0–6 cm) is represented by relatively lower values. The MS values in these intervals start to increase except 11, 20, and 26 cm in Unit-2 (Figure 3). The density profile is almost compatible with the MS curve, implying a positive relationship. While the MS is a useful proxy indicator of changes in the relative intensity of terrigenous input into the lake environment, the most possible reason for low MS values in the core is the high abundance of calcareous fractions in the sediments due to gastropods and mollusc contents.

3.2. Pollen analysis

MT-2 pollen zone (17-1.5 cm depth: 1789 to 1964 AD)

The MT-2 pollen zone is marked by abundant *Pinus brutia* (Turkish pine or Calabrian pine). Apart from pine, the other species seen in the zone in significant amounts is *Pistacia lentiscus* (Figure 4). Warm-temperate forest components in this zone are *Acer* (maple), *Carpinus betulus* (common hornbeam), *Carpinus orientalis* (hornbeam), *Fagus* (beech), *Fraxinus* (ash), *Juglans* (walnut), *Pterocarya* (walnut), deciduous *Quercus* (oak), *Salix* (willow), and *Ulmus* (elm). Within this community, maple, ash, walnut, and elm are only recorded in this pollen zone. The shrubs include olive (*Olea europaea*), evergreen pistachio (*Pistacia lentiscus*), and holm oak (*Quercus ilex*/*coccifera* type). *Pistacia lentiscus* increases towards the bottom of the zone.

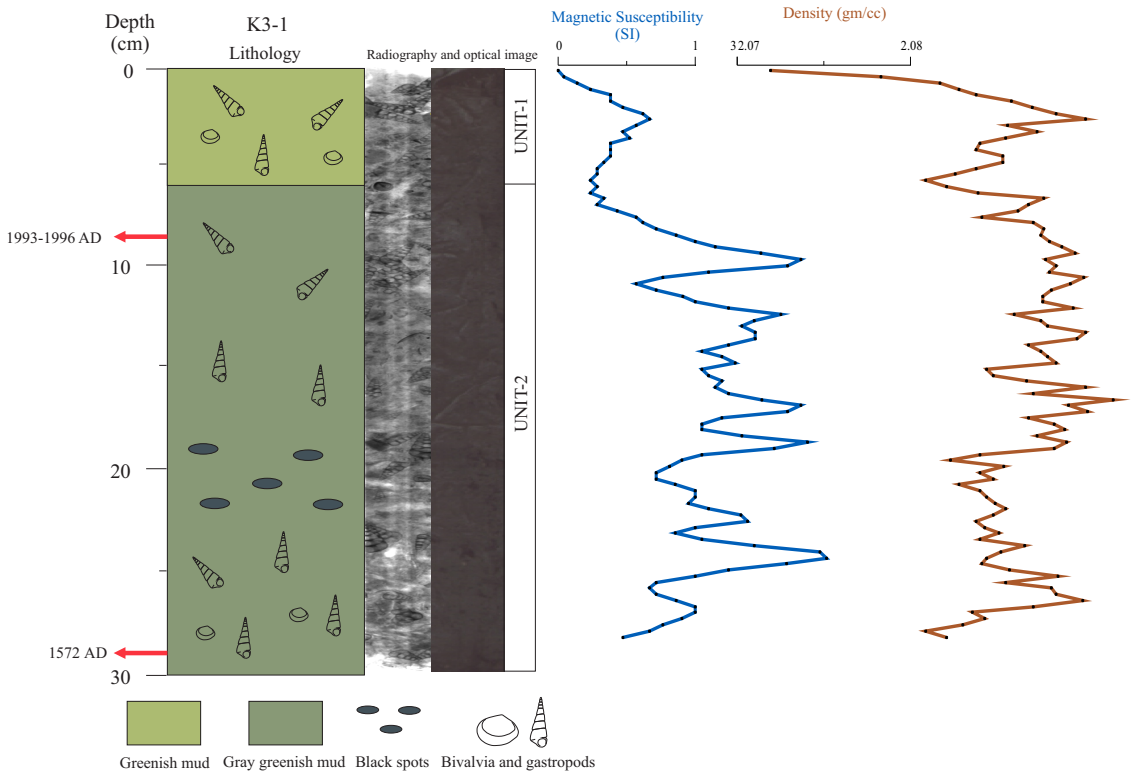

Figure 3. Lithological log radiograph and image of the core with magnetic susceptibility (SI) and density (gm/cc) variation curve.

MT-1 pollen zone (27-17 cm depth: 1613 to 1789 AD)

The pollen zone MT-1 is characterized by the presence of *Pistacia lentiscus*. It increases in this zone and reaches up to 58% at the bottom of the zone (Figure 4). Another prominent pollen grain in this zone is *Pinus brutia* which is notable for its presence in this zone. Trees are composed of only *Carpinus betulus*, deciduous *Quercus*, and *Salix*. *Cedrus* is only seen in this zone with some herbs such as Apiaceae, *Knautia*, Saxifragaceae, and Thymelaea. Among herbs, Amaranthaceae, Asteraceae-Asteroideae, Asteraceae-Cichorioideae, and Poaceae are the most common families. Nonpollen palynomorphs constitute *Glomus*, Pseudoschizaea, Pteridaceae, *Spirogyra* type, Trilete spores, and *Zygnema*.

3.3. Paleontology

The present study also includes bivalvia and gastropods species (Figure 5, Plate I) in the studied sediment core. *Bittium reticulatum* is abundantly present in all samples. *Abra ovata* is frequent at the upper part of the core. *Hydrobia ventrose* occurs in the sediments deposited between 1582 and 1982 AD. The amounts of *Cerastoderma glaucum*, *Mytilus galloprovincialis*, and *Skenea catenoides* are recorded in low abundances (Figure 5).

Family SEMELIDAE Stoliczka, 1870

Abra ovata (Philippi, 1836) (Figure 5, Plate I)

Material examined: lagoon environment, 0–15 cm depth.

Description: Light yellow shell, solid, with rounded-subtriangular shape. The shell is thin, fragile, translucent, and equally valved. Internal margins are crenulated. On the shell, towards the posterior there are numerous longitudinal ribs and concentric lines. **Distribution:** *Abra ovata* is distributed along the coasts of England, the Sea of Marmara, the Adriatic, Black and Azov seas (Vorobyev, 1949). *Abra ovata* is typically also found in the Mediterranean lagoons and estuaries (Kazancı et al., 2003).

Family CERITHIIDAE Fleming, 1822

Bittium reticulatum (da Costa, 1778) (Figure 5, Plate I)

Material examined: lagoon environment, 0–30 cm depth. Needle whelk.

Description: An elongated, conical shell, up to 1 cm long, with 6–7 whorls. Strong ribs and spiral ridges interact to form rows of moderately prominent round elevations (tubercles). Whorls are a little swollen, and the sutures are rather deep. Aperture flared or oval and drawn out to form a short basal sinus. Oval operculum is present. Shell white-gray to light brown in colour.

Distribution: The northeast Atlantic Ocean and the Mediterranean Sea (https://www.sealifebase.ca/summary/Bittium-reticulatum.html).

Family CARDIIDAE Lamarck, 1809

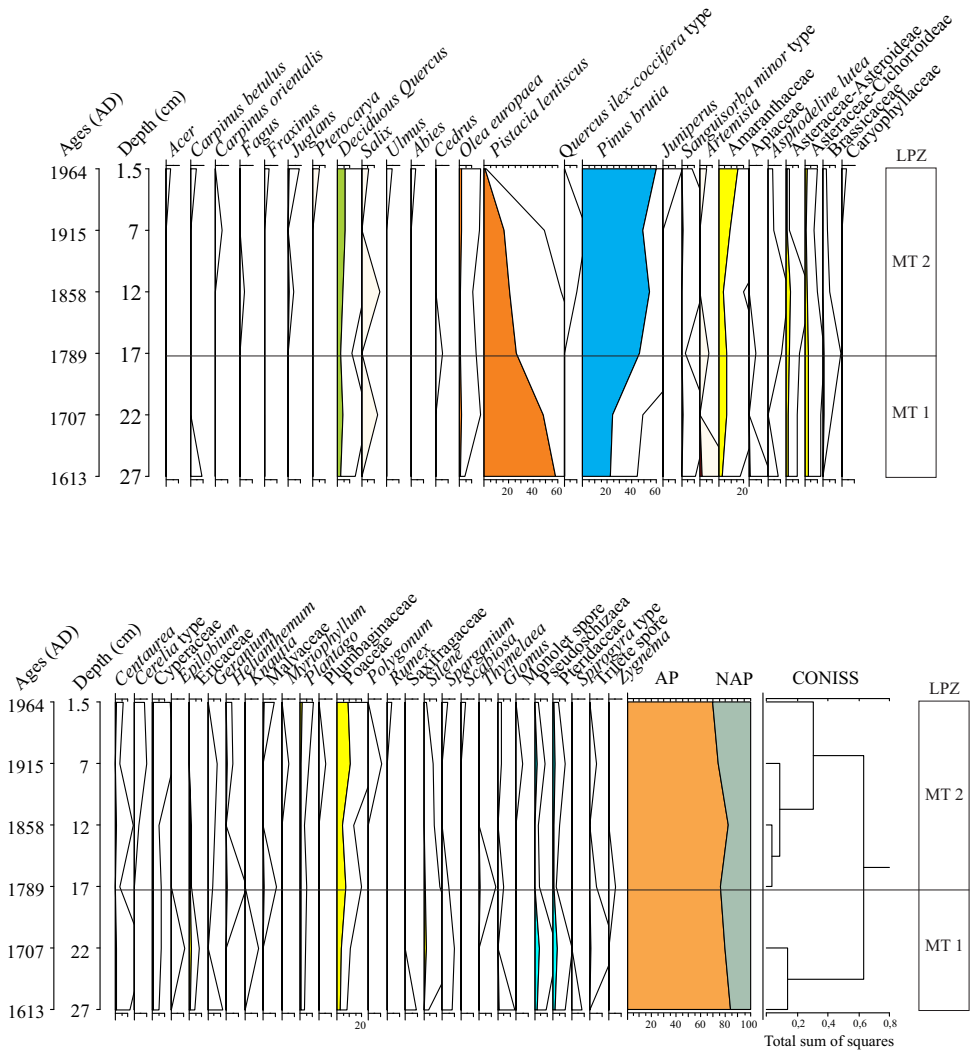

Figure 4. Detailed pollen diagram of the core K3-1. Aquatic plants such as Cyperaceae and *Sparganium* were excluded, but calculated according to total pollen sum. Pollen zones were done using CONISS in TiliaIT program (Grimm, 1987; 1991–2015). Exaggeration curves are ×10. LPZ is the abbreviation of Local Pollen Zone. NAP is the nonarboreal plants, and AP means the arboreal plants.

Cerastoderma glaucum (Bruguière, 1789) (Figure 5, Plate I)

Material examined: lagoon environment, 0–15 cm depth. Lagoon cockle.

Description: Rounded profile over anterior and median areas, a little angular on the posterior slope and low to obsolete on posterior area, yellowish to greenish-brown; some with brownish concentric bands and brownish in the posterior area. Internally white with a brown area over the posterior with this covering the whole of the inner region in some populations, umbo pronounced.

Distribution: The northeast Atlantic, the Mediterranean Sea, and the Caspian Sea. Subtropical to temperate (https://www.sealifebase.ca/summary/Cerastoderma-glaucum.html).

Family MYTILIDAE Rafinesque, 1815

Mytilus galloprovincialis (Lamarck, 1819) (Figure 5, Plate I)

Material examined: lagoon environment, 0–15 cm depth. The Mediterranean mussel.

Description: Two shells are equal and nearly quadrangular. The outside is black-violet coloured; on one side the rim of the shell ends with a pointed and slightly bent umbo while the other side is rounded, although the shell shape varies by region. It also tends to be 5–8 cm.

Distribution: The Mediterranean Sea (Barsotti and Meluzzi, 1968) and the Sea of Marmara, including the Çanakkale and İstanbul straits (Çınar et al., 2020).

Family HYDROBIIDAE Stimpson, 1865

Hydrobia ventrosa (Montagu, 1803) (Figure 5, Plate I)

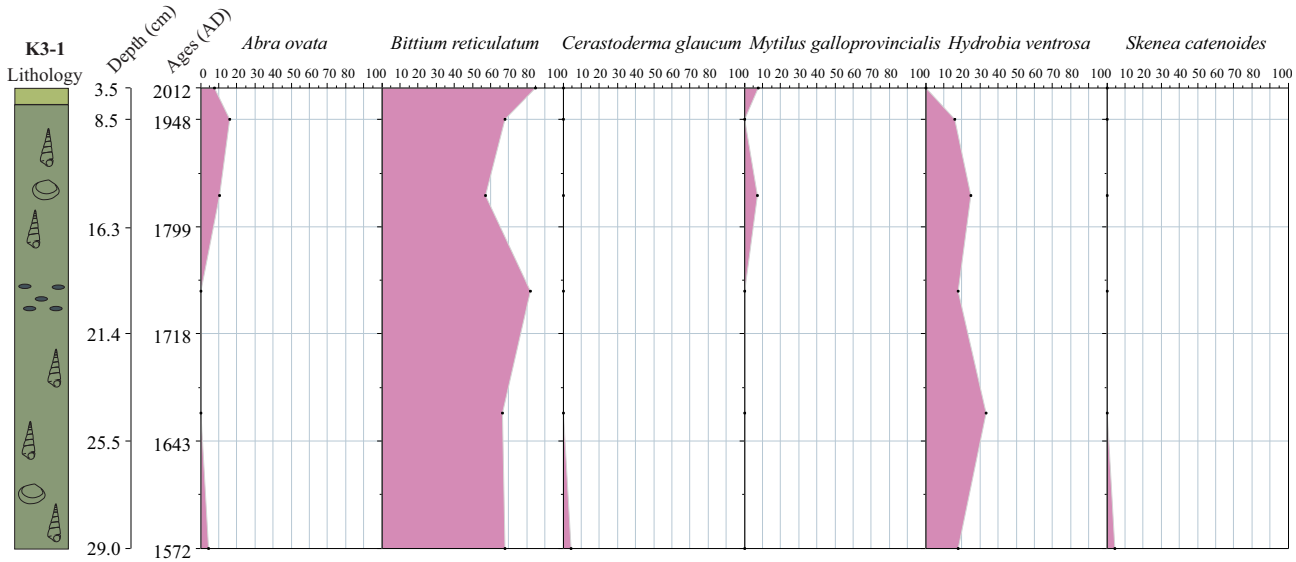

Figure 5. Distribution of bivalvia and gastropod content along the core K3-1 from the Bargilya Cove.

Material examined: lagoon environment, 8–30 cm depth. Mudsnail.

Description: Water snail with a gill and an operculum, an aquatic gastropod mollusk in the family Hydrobiidae. The outside is black-violet coloured; on one side the rim of the shell ends with a pointed and slightly bent umbo while the other side is rounded.

Distribution: The Mediterranean (Barnes et al., 1994) and Black seas (Öktener, 2004).

Family SKENEIDAE Clark W., 1851

Skenea catenoides (Monterosato, 1877) (Figure 5, Plate I)

Material examined: lagoon environment, 30 cm depth. Sea snail.

Description: The size of the shell reaches up to 1.1 mm. The shell is widely umbilicated, closely spirally striated throughout, with several spiral chain-like lines on the base. The whorls are convex, regularly increasing. The outside is black-violet coloured; on one side the rim of the shell ends with a pointed and slightly bent umbo while the other side is rounded, although shell shape varies by region.

Distribution: The central Mediterranean Sea (Giacobbe and Renda, 2018), the Levantine Sea (Öztürk et al., 2014), and the Aegean Sea (Alexopoulos, 2013).

3.4. Geochemical properties of the core

The elemental data have an overall low multivariate correlation. After principal component analysis (PCA) calculations of the variance-covariance matrix on log-transformed XRF data show that the explained variance of the first principal component (PC1) is 25.8%, and the second principal component (PC2) explains 11% (Figure 6). Whereas the first component is dominated among others by Ca, Ti, and K, and subordinately Fe, the second component has high variations in Al and Sr and subordinately Pb. Generally, elements are poorly correlated with each other, e.g., Ca and Ti (r = 0.51). Upcore trends of XRF data expose weakly developed peaks, if at all; for example, values of inc/coh reflecting the organic matter contents range fairly stationary between 4 and 5 (Figure 7). Fe has highest loadings from all elements (0.93 of PC1) and at the same time has low variation when plotted against the sum of all other elements. The Ca/Ti ratio ranges fairly stationary around 2 showing individual peaks at the depths of 27.9, 13.5, and 3 cm. The Sr/Ca ratio ranges mostly between 1 and 4, but it is distinct that the Sr load is increasing towards the upper core half (Figure 7).

4. Discussion

4.1. Reconstructing the vegetation and climate from pollen and geochemical data

The core K3-1 indicates prominent changes in vegetation and climate for the last 400 years. *Pistacia lentiscus* was abundantly recorded in the pollen zone MT-1 between 1613 and 1789 AD. After this time, the amount of *P. lentiscus* decreases and reaches down to ca. 26%. During this time, *Pinus brutia* appears to increase at the upper part of the pollen zone MT-1 (Figures 4 and 7). *P. lentiscus* is a mastic tree and belongs to the Anacardiaceae family. It is distributed along the Mediterranean region including Turkey, Italy, Morocco, Greece, and the Iberian Peninsula (Ak and Parlakçı, 2009). In Turkey, it is found in seaside stony areas and/or in historical ruins (Ak and Parlakçı, 2009). It is used commercially for gum from the trunk (Ak and Parlakçı, 2009). It can tolerate harsh climate conditions and can live under a maximum temperature of 45 °C (Kozhoridze et al., 2015). *Pistacia* indicates its highest values in the pollen zone MT-1. The nonarboreal plants

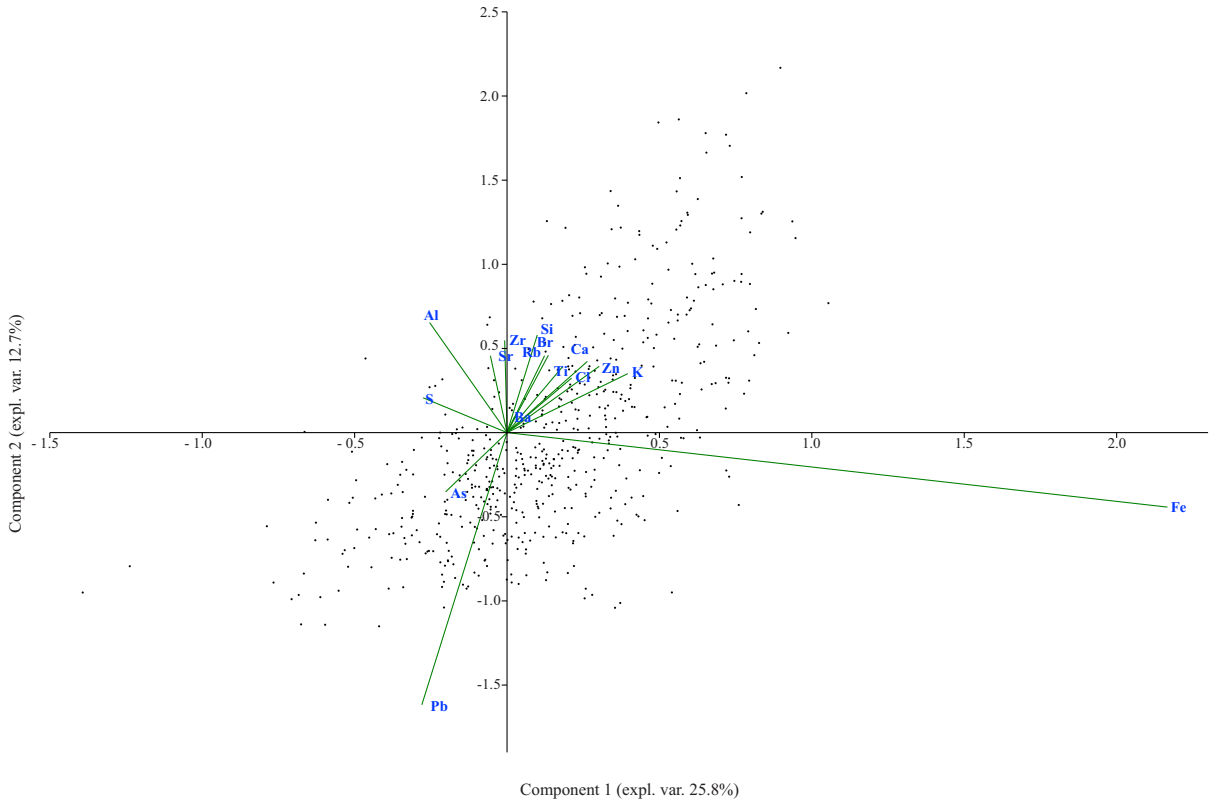

Figure 6. Biplot (PC1-PC2) showing element correlations and data point distributions of log-ratio transformed XRF element intensity data. The data set shows the strongest positive PC1-loadings for the elements Ca, Ti, K, and Fe are separated from them with negative loadings on their PCA2- axis likely related to subaquatic redox conditions. Al and Sr have the most pronounced negative loadings on the PC1 axis possibly pointing to a subordinate source rock geology and with Pb as a counterpart that is the only element with double negative loadings on both PC1 and PC2 axis. This might be due to biomineralization or independent detrital input from bedrock.

(NAP) values are generally low, and the arboreal plants (AP) values are high in the whole diagram. Anthropogenic indicators, such as *Olea europeae*, may suggest slight agricultural activities between 1613 and 1789 AD.

Other forest components are deciduous forest, including *Carpinus betulus*, deciduous *Quercus*, *Salix*, and some Mediterranean trees, such as *Olea europaea*. *Cedrus* was only present in this pollen zone with less amount. This indicates that cedar trees have been transported from the upslopes of middle elevations. Within herbaceous assemblages, Amaranthaceae, Asteraceae-Asteroideae, Asteraceae-Cichorioideae, and Poaceae are prominently represented. Pteridaceae spores are present as well in the zone. Nonpollen palynomorphs constitute *Glomus*, Pseudoschizaea, and *Spirogyra* type.

At the beginning of the pollen zone MT-2, agricultural activities increase once again. The amount of *Pistacia lentiscus* drops while *Pinus brutia* increases in this zone between 1789 and 1964 AD. Primary anthropogenic indicators, including *Olea europeae* and *Juglans*, are present in the pollen zone MT-2. Open land vegetation is characterized by Amaranthaceae, Asteraceae-Asteroideae, Asteraceae-Cichorioideae, and Poaceae. They are spread due to woodcutting. The occurrence of *Plantago*, Caryophyllaceae, *Cerelia*, *Rumex*, *Sanguisorba minor* type, and *Scabiosa* may indicate the increasing importance of pastoralism and agriculture between 1789 and 1964 AD. A high abundance of *Pinus brutia* can be due to the increasing transportation of pine pollen into the open lands and/or climate and human effect between 1789 and 1964 AD. In Turkey, *Pinus brutia* is a drought-tolerant plant (Kandemir et al., 2017). Red pines are mainly used in resin production, construction materials, agricultural tools, wood wire poles, mine poles, fence posts, shipbuilding, and paper industry (Bozkurt, 1971, 1982; Erten and Taşkın, 1985; Öktem, 1987; Tolunay et al., 2008). Some slight changes in the Sr-Ca ratio suggest a connection with climate when compared with the pollen data. *Pinus brutia* variation behaves in a parallel way to the Sr-Ca ratio (Figure 7). When the Sr-Ca ratio increases in the upper core half, the abundance of pine trees also increases. On the contrary, the percentage of *Pistacia* pollen decreases

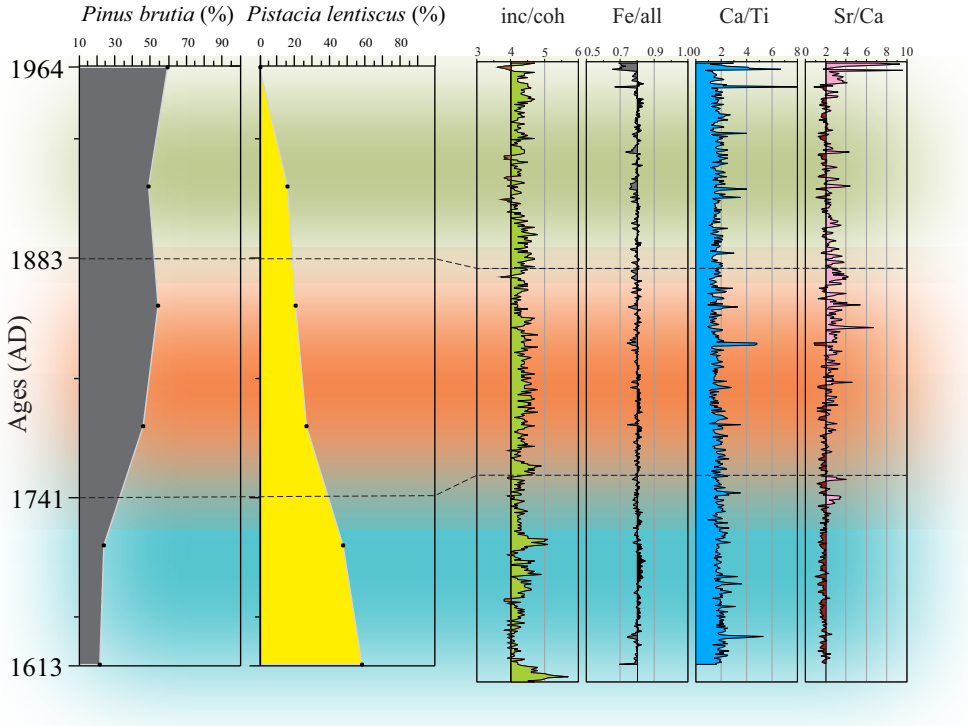

Figure 7. Radiograph, core image, lithostratigraphy, and downcore plots from XRF core scanning of the Bargilya Cove K3 sediment sequence. The selected properties are the Compton (incoherent) and Rayleigh (coherent) scattering ratios, Fe/all, Ca/Ti and Sr/Ca ratios with comparison of *Pistacia lentiscus* and *Pinus brutia* pollen grains.

where the Sr-Ca ratio increases. In fact, the mastic tree is a drought-resistant plant, its percentage still decreases. It can be said that the factor affecting the amount of *Pistacia* might be the change in the amount of precipitation rather than the temperature.

Although *Pistacia lentiscus* is resistant to the winter temperatures (Larcher, 2000), a decrease in water availability during the summer season is the affecting factor for an expansion of pistachio and also causes mortality of *P. lentiscus* seedlings (Garcia-Fayos and Verdú, 1998). It seems that the distribution of pistachio depends on high winter temperatures and frequent and heavy rain (Jordano, 1989). Therefore, the expansion of *P. Lentiscus* from 1613 AD to 1789 AD (27-17 cm) in the core may indicate relatively high winter temperatures and frequent and heavy rains. In the pollen zone MT-2, a decline in the abundance of *P. lentiscus* may be a result of an abrupt decrease in moisture availability. The low appearance of *Fagus* pollen may be due to long-distance transportation. Some riparian forest also develops including *Salix* and *Ulmus* around the Bargilya Cove after 1915 AD.

Complementary detrital and authigenic signals of sediment origin are preserved in XRF data and support the interpretation of sediment environments (e.g., Çağatay et al., 2019, Löwemark et al., 2019, Schwamborn et al., 2020). For the upper levels of Bargilya Cove sediments, the XRF data suggest an overall homogeneous composition. PCA analysis is an important tool to separate common signals within a complex dataset. We have applied a PCA on the K3-1 sediment record, including 16 elements. According to the XRF data, sediment change is faintly expressed using the (inc/coh) ratio and the Ca behaviour. The (inc/coh) ratio as a proxy for organic carbon contents points to a fairly organic-rich environment with total organic contents of 10%–20% and corresponding loss-on-ignition (LOI) 550 °C values of 20% to 30% following Chawchai et al. (2016). Ca, K and Si elements well correlate with Ti, suggesting that these elements indicate a detrital input (Kylander et al., 2011). As all four of these elements group together in the PCA (Figure 6) and follow similar patterns. However, detrital signals, such as Ti and Fe, do not show distinct trends along the core. High counts of Fe thereby might be related to redox conditions that are typical for a subaquatic environment; Fe has an average of 80% of all counts per second (cps), and it is the dominating signal. Grey-greenish colours for much of the short core rather indicate an anoxic environment, which favours the interpretation that iron is likely to present as Fe^{2+}. Pb shows an independent behaviour (Figure 6), although it is not trending over the record and remains at low counts.

It may suggest a link to biomineralization (Ehrlich et al., 2021), but remains speculative until further notice. The Sr/Ca ratio is a proxy for Sr uptake by $CaCO_3$ forming organisms (Rothwell et al., 2006). The correlation between Ca and Sr between 1613 and 1741 AD is low, indicating that carbonate precipitation is not an important factor during this time interval. However, after 1741 AD, corelation between Ca and Sr is very strong based on the primary component analysis PC-1 and PC-2. Higher values in Ca/Ti and Sr/Ca may indicate alkaline environment under semiarid conditions (Hughes-Allen et al., 2021). An increase in Sr/Ca ratio in the upper level of Unit 1 may be related to the existence of alkaline environment during the deposition of this unit. Low precipitation and/or strong summer insolation may cause evaporation. Also, this is supported by pollen data. The amount of *Pistacia lentiscus* decreases due to the increased evaporation in the upper level of the core.

The composition of macrobenthic mollusc includes *Abra ovata*, *Bittium reticulatum*, *Cerastoderma glaucum*, *Mytilus galloprovincialis*, *Hydrobia ventrosa*, and *Skenea catenoides* (Figure 5). *Bittium reticulatum* and *Hydrobia ventrosa* are distributed in almost all samples. The bivalve *Abra ovata* are abundant in the first levels of the core, especially in 1982. *Bittium reticulatum* is a marine species while *Cerastoderma glaucum* and *Abra Ovata* are typical inhabitants of brackish waters (Barnes, 1980). *Abra ovata*, *Cerastoderma glaucum*, *Mytilus galloprovincialis*, and *Hydrobia ventrosa* are eusterine species. *Skenea catenoides* are only observed between 1572and 1643 AD.

Abra ovata, *Cerastoderma glaucum*, *Bittium reticulatum*, and *Skenea catenoides* are the pioneer settlers in the Güllük Bay between 1572 and 1643 AD. The last appearance of *Cerastoderma glaucum* and *Skenea catenoides* occur at 1643 AD. The interval of 16.3–8.5 cm (1799–1948 AD) is characterised by a clear shift in mollusc population (Figure 5). Lagoonal species *Abra ovata* and *Hydrobia ventrosa* increase, whereas the number of marine species *Bittium recticulatum* decreases between 1799 and 1948 AD. This may indicate a change in environmental conditions (such as salinity, temperature, nutrients) from a lagoonal depositional environment with marine influence to a more isolated lagoonal environment. This shift may result from local paleomorphological changes such as a closure of the connections between the lagoon and the sea. After 1948 AD, *Bittium reticulatum* increases while the amount of lagoonal species *Abra ovata* and *Hydrobia ventrosa* decrases. This suggests that marine influence occurs again in the region.

5. Conclusion

The sediment core from the Bargilya Cove indicates the changes in vegetation and climate using multiproxy analysis during the last 400 years. Forest components compose of mainly *Pistacia lentiscus* shrubs between 1613 and 1741. However, schrub level is replaced by *Pinus brutia* after 1707 AD. An increase in pine has continued until 1964 AD whereas *Pistacia* forest sharply drop in the pollen zone MT-2. This situation is well recorded in the Sr-Ca ratio. The values of Sr-Ca increase in the upper part of the core, reclecting more arid conditions were prevailing in the region. This suggests that the presence of *Pistacia* is likely related to decreasing precipitation rather than temperature. The remaining forest communities cover deciduous trees and evergreen coniferous trees such as *Carpinus betulus*, *C. orientalis*, *Fagus*, deciduous *Quercus*, *Fraxinus*, *Juglans*, and *Pterocarya* with riparian *Salix* and *Ulmus* forest.

Summarizing and with regard to the distribution of molluscs in the Bargilya Cove, the presence of *Abra ovata*, *Bittium reticulatum*, *Cerastoderma glaucum*, *Mytilus galloprovincialis*, *Hydrobia ventrosa*, and *Skenea catenoides* points to a marine species composition, which also is capable of living in the mild transitional zone between the estuarine and the marine environment.

Acknowledgements

This study has been produced benefiting from the 2232 International Fellowship for Outstanding Researchers Program of the Scientific and Technological Research Council of Turkey (TÜBİTAK) through grant 118C329. The financial support received from TÜBİTAK does not indicate that the content of the publication is approved in a scientific sense by TÜBİTAK.

References

Aitchison J (1990). Relative variation diagrams for describing patterns of compositional variability. Mathematical Geology 22: 487–511. doi: 10.1007/BF00890330

Akyol, Y (2009). Kıyı Ege'nin (Edremit Körfezi-Gökova Körfezi arası) vejetasyon ekolojisi ve biyolojik çeşitliliğinin ekolojik yönetimi. Ege Üniversitesi Fen Bilimleri Enstitüsü. Doktora Tezi. 268 pages (in Turkish).

Alexopoulos AA (2013). The Gastropods (Clams) of the Greek Seas. University of Thessaly. Diploma/Degree Thesis, 176 pages (in Greek).

Altınsaçlı S, Perçin-Paçal F, Altınsaçlı S (2015). Assessments on diversity, spatiotemporal distribution and ecology of the living ostracod species (Crustacea) in oligo-hypersaline coastal wetland of Bargilya (Milas, Muğla, Turkey). International Journal of Fisheries and Aquatic Studies 3 (2): 357–373.

Barnes RSK (1980). Coastal lagoons. The natural history of a neglected habitat. Cambridge: Cambridge University Press. Cambridge Studies in Modern Biology, no. 1, 106 p.

Barnes RJ, Barnes RSK (1994). The Brackish-Water Fauna of Northwestern Europe. Cambridge University Press, 287 pages.

Barsotti G, Meluzzi C (1968). Osservazioni su Mytilus edulis L. e Mytilus galloprovincialis Lamark.). Conchiglie 4:50–58 (in Italian).

Biltekin D, Eriş K, Çağatay N, Akçer Ön S, Bal Akkoca D (2018). Late Pleistocene-Holocene environmental change in eastern Turkey: multiproxy palaeoecological data of vegetation and lake-catchment changes. Journal of Quaternary Science 33 (5): 575–585. doi: 10.1002/jqs.3037

Biltekin D, Eriş KK, Bulut S (2021). Anthropogenic influences and climate changes in Lake Hazar (eastern Turkey) during the Late Holocene. Quaternary International 583: 70–82. doi: 10.1016/j.quaint.2021.02.023

Blaauw M (2010). Methods and code for 'classical'age-modelling of radiocarbon sequences. Quaternary Geochronology 5 (5): 512–518. doi: 10.1016/j.quageo.2010.01.002.

Bottema S, Woldring H (1984). Late Quaternary vegetation and climate of southwestern Turkey. Paleohistoria 26: 123–149.

Bottema S (1995). Holocene vegetation of the Van area: palynological and chronological evidence from Söğütlü, Turkey. Vegetation History and Archeobotany 4: 187–193. doi: 10.1007/BF00203937

Bozkurt Y (1971). Önemli Bazı Ağaç Türleri Odunlarının Tanımı Teknolojik özellikleri ve Kullanış Yerleri. İstanbul Üniversitesi, Orman Fakültesi Yayını, No: 177 (in Turkish).

Bozkurt Y (1982). Ağaç Teknolojisi. İstanbul Üniversitesi, Orman Fakültesi Yayını, No: 296 (in Turkish).

Cohen AS (2003). Paleolimnology, the History and Evolution of Lake Systems. Oxford University Press, p. 500

Çağatay MN, Öğretmen N, Damcı E, Stockhecke M, Sancar Ü et al. (2014). Lake level and climate records of the last 90 ka from the Northern Basin of Lake Van, eastern Turkey. Quaternary Science Reviews 104: 97–116. doi: 10.1016/j.quascirev.2014.09.027

Çağatay MN, Wulf S, Sancar Ü, Özmaral A, Vidal L et al. (2015). The tephra record from the Sea of Marmara for the last ca. 70 ka and its palaeoceanographic implications. Marine Geology 361: 96–110. doi: 10.1016/j.margeo.2015.01.005

Chawchai S. Kylander ME, Chabangborn A, Löwemark L, Wohlfarth B (2016). Testing commonly used X-ray fluorescence core scanning-based proxies for organic-rich lake sediments and peat. Boreas 45: 180–189. doi: 10.1111/bor.12145

Conde D, Bonilla S, Aubriot L, de Léon R, Pintos W (1999). Comparison of the areal amount of chlorophyll a of planktonic and attached microalgae in a shallow coastal lagoon. Hydrobiologia 408/409: 285–291. doi: 10.1023/A:1017086513787

Cour P (1974). Nouvelles techniques de détection des flux et des retombées polliniques: étude de la sédimentation des pollens et des spores à la surface du sol. Pollen et Spores 16: 103–141.

Croudace IW, Rindby A, Rothwell RG (2006). ITRAX: description and evaluation of a new multi-function X-ray core scanner. Geological Society, London, Special Publications 267 (1): 51–63. doi: 10.1144/GSL.SP.2006.267.01.04

Cugny C, Mazier F, Galop D (2010). Modern and fossil non-pollen palynomorphs from the Basque mountains (western Pyrenees, France): The use of coprophilous fungi to reconstruct pastoral activity. Vegetation History and Archaeobotany 19: 391–408. doi: 10.1007/s00334-010-0242-6

Çınar ME, Bakır K, Öztürk B, Doğan A, Açık Ş et al. (2020). Spatial distribution pattern of macroinvertebrates associated with the black mussel Mytilus galloprovincialis (Mollusca: Bivalvia) in the Sea of Marmara. Journal of Marine Systems 211: 103402. doi: 10.1016/j.jmarsys.2020.103402

Danladi İB, Akçer Ön S, Ön ZB, Schmidt S (2021). High-resolution temperature and precipitation variability of southwest Anatolia since 1730 CE from Lake Gölcük sedimentary records. Turkish Journal of Earth Sciences 30: 601–610. doi: 10.3906/yer-2008-14

Eastwood WJ, Roberts N, Lamb HF, Tibby JC (1999). Holocene Environmental Change in Southwest Turkey: a Palaeoecological Record of Lake and Catchment-Related Changes. Quaternary Science Reviews 18: 671–695. doi: 10.1016/S0277-3791(98)00104-8

Dean JR, Jones MD, Leng MJ, Noble SR, Metcalfe SE et al. (2015). Eastern Mediterranean hydroclimate over the late glacial and Holocene, reconstructed from the sediments of Nar lake, central Turkey, using stable isotopes and carbonate mineralogy. Quaternary Science Reviews 124: 162–174. doi: 10.1016/j.quascirev.2015.07.023.

Ehrlich H, Bailey E, Wysokowski M, Jesionowski T (2021). Forced Biomineralization: A Review. Biomimetics 6 (3): 46. doi: 10.3390/biomimetics6030046

Eriş K (2013). Late Pleistocene-Holocene sedimentary records of climate and lake-level changes in Lake Hazar, eastern Anatolia, Turkey. Quaternary International 302: 123–134. doi: 10.1016/j.quaint.2012.12.024

Eriş KK, Akçer Ön S, Çağatay MN, Ülgen UB, Ön ZB et al. (2017). Late Pleistocene to Holocene paleoenvironmental evolution of Lake Hazar, Eastern Anatolia, Turkey. Quaternary International 486: 4–16. doi: 10.1016/j.quaint.2017.09.027

Eriş KK, Arslan TN, Sabuncu A (2018b). Influences of climate and tectonic on the middle to late Holocene deltaic sedimentation in lake hazar, eastern Turkey. Arabian Journal for Science and Engineering 43: 3685–3697. doi: 10.1007/s13369-017-3021-1

Erten P, Taşkın O (1985). Kızılçam (Pinus brutia Ten) Kabuklarında Tanen Miktarının Saptanmasına ilişkin Araştırmalar. Ormancılık Araştırma Enstitüsü Yayınları, Teknik Bülten Serisi, No: 135.

Fleitmann D, Cheng H, Badertscher S, Edwards RL, Mudelsee M et al. (2009). Timing and climatic impact of Greenland interstadials recorded in stalagmites from northern Turkey. Geophysical Research Letters 36 (19): L19707. doi: 10.1029/2009GL040050

Garcia-Fayos P, Verdu´ M (1998). Soil seed bank, factors controlling germination and establishment of a Mediterranean shrub: Pistacia lentiscus. L. Acta Oecologica 19: 357–366. doi: 10.1016/S1146-609X(98)80040-4

Gelorini V, Verbeken A, van Geel B, Cocquyt C, Verschuren D (2011). Modern non-pollen palynomorphs from East African lake sediments. Review of Palaeobotany and Palynology 164: 143–173. doi: 10.1016/j.revpalbo.2010.12.002

Grimm EC (1987). CONISS: a Fortran 77 program for stratigraphically constrained cluster analysis by the method of incremental sum of squares. Computers & Geosciences 13: 13–35. doi: 10.1016/0098-3004(87)90022-7

Hughes-Allen L, Bouchard F, Hatté C, Meyer H, Pestryakova LA, Diekmann B, Subetto DA, Biskaborn BK (2021). 14,000-year carbon accumulation dynamics in a Siberian lake reveal catchment and lake productivity changes. Frontiers in Earth Science 9: 710257. ff10.3389/feart.2021.710257ff.

Jones MD, Roberts CN, Leng MJ (2007). Quantifying climatic change through the last glacial–interglacial transition based on lake isotope palaeohydrlogy from central Turkey. Quaternary Research 67: 463–473. doi: 10.1016/j.yqres.2007.01.004

Jordano P (1989). Pre-dispersal biology of Pistacia lentiscus (Anacardiaceae): cumulative effects on seed removal by birds. Oikos 55: 375–386. doi: 10.2307/3565598

Kamar G (2018). Palynology of lake Arin (eastern Anatolia, Turkey) deposits and its relation with water level change of lake van: preliminary findings. Quaternary International 486: 83–88. doi: 10.1016/j.quaint.2017.05.020.

Kandemir G, Önde S, Temel F, Kaya Z (2017). Population variation in drought resistance and its relationship with adaptive and physiological seedling traits in Turkish red pine (Pinus brutia Ten.). Turkish Journal of Biology 41: 256-267. doi: 10.3906/biy-1608-77

Karadaş A (2013). Bornova Ovası Kıyı Sedimanlarında Palinolojik Analizler. Prof. Dr. İlhan KAYAN'a Armağan, Editör: ÖNER, E. İzmir: Ege Üniversitesi Yayınları. Edebiyat Fakültesi Yayın No: 181 (in Turkish).

Karlıoğlu Kılıç NK, Caner H, Erginal AE, Ersin S, Selim HH et al. (2018). Environmental changes based on multi-proxy analysis of core sediments in Lake Aktaş Turkey: Preliminary results. Quaternary International 486: 89–97. doi: 10.1016/j.quaint.2018.02.004

Kazancı N, Oguzkurt D, Girgin S, Dügel M (2003). Distribution of benthic macroinvertebrates in relation to physico-chemical properties in the Köyceğiz-Dalyan Estuarine Channel System (Mediterranean Sea, Turkey). Indian Journal of Marine Science 32 (2):141–146.

Kjerfve B (Editor) (1994). Coastal lagoon processes. Elsevier Oceanographic Series, Amsterdam, 1–8.

Kuzucuoğlu C, Dörfler W, Kunesch S, Goupille F (2011). Mid- to late-Holocene climate change in central Turkey: The Tecer Lake record. The Holocene 21 (1): 173–188. doi: 10.1177/0959683610384163

Kylander ME, Ampel L, Wohlfarth B, Veres D (2011). High-resolution X-ray fluorescence core scanning analysis of Les Echets (France) sedimentary sequence: New insights from chemical proxies. Journal of Quaternary Science 26: 109–117. doi: 10.1002/jqs.1438

Larcher W (2000). Temperature stress and survival ability of Mediterranean sclerophyllous plants. Plant Biosystems 134: 279–295. doi: 10.1080/11263500012331350455

Litt T, Krastel S, Sturm M, Kipfer R, Örçen S et al. (2009). 'PALEOVAN', International Continental Scientific Drilling Program (ICDP): site survey results and perspectives. Quaternary Science Reviews 28: 1555–1567. doi: 10.1016/j.quascirev.2009.03.002

Löwemark L, Bloemsma M, Croudace I, Daly JS, Edwards RJ et al. (2019). Practical guidelines and recent advances in the Itrax XRF core-scanning procedure. Quaternary International 514: 16–29. doi: 10.1016/j.quaint.2018.10.044

Luterbacher J, García-Herrera R, Sena Akcer-On S, Allan R, Alvarez-Castro MC et al. (2012). A Review of 2000 Years of Paleoclimatic Evidence in the Mediterranean. The Climate of the Mediterranean Region. Edited by P. Lionello. 2012, Pages 87–185.

Nixon SW (1982). Nutrients dynamics, primary production and fisheries yields of lagoons. Oceanologica Acta, 357–371.

Ocakoğlu F, Kır O, Yılmaz İÖ, Açıkalın S, Erayık C et al. (2013). Early to Mid-Holocene Lake level and temperature records from the terraces of Lake Sünnet in NW Turkey. Palaeogeography, Palaeoclimatology, Palaeoecology 369: 175–184. doi: 10.1016/j.palaeo.2012.10.017

Öktem E (1987). Kızılçam. Ormancılık Araştırma Enstitüsü Yayınları, El Kitabı Dizisi 2, yayın serisi 52: 182 pages (in Turkish).

Öktener A (2004). A preliminary research on mollusca species of some freshwaters of Sinop and Bafra. Gazi University. Journal of Science 17 (2): 21–30.

Öztürk B, Doğan A, Bitlis Bakır B, Salman A (2014). Marine molluscs of the Turkish coasts: an updated checklist. Turkish Journal of Zoology 38: 832-879. doi: 10.3906/zoo-1405–78

Reille M (1992). Pollen et spores d'Europe et d'Afrique du Nord. Laboratoire de botanique historique et de palynologie, Marseille, France. 543 pp.

Reimer PJ, Austin WEN, Bard E, Bayliss A, Blackwell PG et al. (2020). The IntCal20 northern hemisphere radiocarbon age calibration curve (0–55 cal kBP). Radiocarbon 62 (4): 725–757. doi: 10.1017/RDC.2020.41.

Reimer PJ, McCormac FG (2002). Marine radiocarbon reservoir corrections for the Mediterranean and Aegean seas. Radiocarbon 44 (1): 159–166. doi: 10.1017/S0033822200064766

Roberts N, Jones MD, Benkaddour A, Eastwood WJ, Filippi ML et al. (2008). Stable isotope records of Late Quaternary climate and hydrology from Mediterranean lakes: the ISOMED synthesis. Quaternary Science Reviews 27: 2426–2441. doi: 10.1016/j.quascirev.2008.09.005

Roberts N, Brayshaw D, Kuzucuoğlu C, Perez R, Sadori L (2011a). The Mid-Holocene Climatic Transition in the Mediterranean: Causes and Consequences. The Holocene 21 (1): 3–13. doi: 10.1177/0959683610388058

Roberts N, Eastwood WJ, Kuzucuoğlu C, Fiorentino G, Caracuta V (2011b). Climatic, vegetation and cultural change in the eastern Mediterranean during the mid-Holocene environmental transition. The Holocene 21: 147–162. doi: 10.1177/0959683610386819

Roberts N (Editor) (2014). The Holocene: An Environmental History. Wiley–Blackwell, USA, 3rd Edition, 378 pages.

Rothwell RG, Hoogakker B, Thomson J, Croudace IW, Frenz M (2006). Turbidite Emplacement on the Southern Balearic Abyssal Plain (Western Mediterranean Sea) during Marine Isotope Stages 1-3: an Application of ITRAX XRF Scanning of Sediment Cores to Lithostratigraphic Analysis. Geological Society Special Publication. doi: 10.1144/GSL.SP.2006.267.01.06

Russell AD, Hönisch B, Spero HJ, Lea DW (2004). Effects of seawater carbonate ion concentration and temperature on shell U, Mg, and Sr in cultured planktonic foraminifera. Geochimica et Cosmochimica Acta 68 (21): 4347-4361. doi: 10.1016/j.gca.2004.03.013

Schöne BR, Zhanga Z, Radermacher P, Thébault J, Jacob DE et al. (2011). Sr/Ca and Mg/Ca ratios of ontogenetically old, long-lived bivalve shells (Arctica islandica) and their function as paleotemperature proxies. Palaeogeography, Palaeoclimatology, Palaeoecology 302 (1–2): 52–64. doi: 10.1016/j.palaeo.2010.03.016

Schwamborn G, Hartmann K, Wünnemann B, Rösler W, Berke MA et al. (2020). Sediment history mirrors Pleistocene aridification in the Gobi Desert (Ejina Basin, NW China). Solid Earth, 11 (4): 1375–1398, doi: 10.5194/se-11-1375-2020.

Sullivan DG (1989). Human Induced Vegetation Change in Western Turkey: Pollen Evidence from Central Lydia. PhD Thesis, University of California, Berkeley.

Tolunay A, Akyol A, Özcan M (2008). Usage of Trees and Forest Resources at Household Level: A Case Study of Asağı Yumrutaş Village from the West Mediterranean Region of Turkey. Research Journal of Forestry 2(1): 1–14. doi: 10.3923/rjf.2008.1.14

Ülgen UB, Oliver Franz S, Biltekin D, Çağatay MN, Roeser PA et al. (2012). Climatic and environmental evolution of the Lake Iznik (NW Turkey) over the last ~4700 years. Quaternary International 274: 88–101. doi: 10.1016/j.quaint.2012.06.016

van Geel B, Aptroot A, Mauquoy D (2006). Sub-fossil evidence for fungal hyperparasitism (Isthmospora spinosa on Meliola ellisii, on Calluna vulgaris) in a Holocene intermediate ombrotrophic bog in northern-England. Review of Palaeobotany and Palynology 141: 121–126. doi: 10.1016/j.revpalbo.2005.12.004

van Zeist W, Woldring H, Stapert D (1975). Late Quaternary Vegetation and Climate of Southwestern Turkey. Palaeohistoria 17: 53–143.

van Zeist W, Woldring H (1978). A postglacial pollen diagram from Lake Van in east Anatolia. Review of Palaeobotany and Palynology 26: 249–276. doi: 10.1016/0034-6667(78)90015-5

van Zeist W, Bottema S (1991). Late Quaternary vegetation of the Near East. Beihefte zum Tübinger Atlas Des Vorderen Orients Reihe A (Naturwissenschaften) Nr. 18, Dr. Ludwig Reichert Verlag, Wiesbaden.

Vorobyev VP (1949). A Benthos of Azov Sea. In: Trudy Azovo-Chernomorskogo Inst. morsk. rybnogo hozyaistva i okeanografii, Izd. Pischevaya promyshlennost.

Weaver PPE, Schultheiss PJ (1990). Current methods for obtaininig, logging and splitting marine sediment cores. Marine Geophysical Researches 12: 85–100.

Wick L, Lemcke G, Strum M (2003). Evidence of Lateglacial and Holocene climatic change and human impact in eastern Anatolia: high resolution pollen, charcoal, isotopic and geochemical records from the laminated sediments of Lake Van, Turkey. The Holocene 13 (5): 665–675. doi: 10.1191/0959683603hl653rp

Woodbridge J, Roberts N (2011). Late Holocene climate of the Eastern Mediterranean inferred from diatom analysis of annually-laminated lake sediments. Quaternary Science Reviews 30: 3381–3392. doi: 10.1016/j.quascirev.2011.08.013